# Validation of a CFD Study of Particle Distribution in Nuclear Workplace

P. Geraldini[1]
[1] Sogin spa, Via Marsala 51C 00185 Rome - Italy, geraldini@sogin.it

**Abstract:** In nuclear work environments where contaminated materials are handled there is always a possibility of accidental airborne releases of toxic or radioactive substances in form of aerosols and gases. Because of that, safety professionals and engineers are required to design effective warning systems and countermeasures to minimize a worker's risk. Understanding the air flows patterns and aerosol trajectories in ventilated rooms can provide key information for determining where to place early warning and monitoring instruments, and how to minimize hazardous materials in the worker's breathing zone. In particular, with the numerical simulations, they have been firstly evaluated the capabilities of the numerical model to reproduce the available experimental data and secondly defined a strategy for positioning of continuous air monitoring to obtain a quickly and good sensitive response. The 3D simulations have been performed with COMSOL Multiphysics version 5.2 (Heat Transfer and Particle Tracing Modules).

**Keywords:** CFD, particle tracing, nuclear, contamination, monitoring system.

## 1. Introduction

Accidental release of toxic material could occur in nuclear work environments where contaminated materials are handled. In such facilities are normally used real-time air monitoring, the Continuous Air Monitors (CAM), placed in occupied work areas where an individual is likely to receive a dose of ionizing radiation which exceeds the limits (Derived Air Concentration-hours). In addition, CAMs are needed where there is a necessity to alert individuals to unexpected increases in airborne radioactivity.

Knowledge of aerosol or gas dispersion patterns in work areas is important to ensuring the CAM are located in quantities and in positions that provide adequate worker protection, also considering the high cost of each CAM. The dispersion within rooms can be influenced by complex interactions between numerous variables, but especially ventilation design and room furnishings. In fact, the assumption of a well mixed condition of room air and particles could fail because perfect mixing is difficult to obtain. In order to accurately design a healthy indoor environment, it is important to consider spatial distributions of particles.

The reference experimental benchmark studied the dependence of ventilation rate and furnishings on aerosol dispersion within a room that was designed to approximate a plutonium laboratory (glove box facility).

A Lagrangian CFD numerical model has been implemented to evaluate a ventilation-system-induced flow field, calculate aerosol dispersion, benchmark the model with experimental measurements, and to define the optimized positioning of CAM to obtain a quickly and good sensitive response. Two ventilations rates and three different release locations were numerically studied. The 3D simulations have been performed with COMSOL Multiphysics version 5.2 (Heat Transfer and Particle Tracing Modules).

Although the overall computational cost is considerable, the numerical results agree well with associated experimental data. The development of this work has allowed us to obtain useful indications for designing a Continuous Air Monitoring sampling layout.

## 2. Glove-box characteristics

A glove box is a large enclosure used in nuclear facilities to perform laboratory operations safely. Built into the sides of the glove-box are gloves arranged in such a way that the user can place their hands into the gloves and perform tasks inside the box without breaking containment. Part or all of the box is usually transparent to allow the user to see what is being manipulated. Glove boxes are typically operated at a negative differential pressure to laboratory to preclude leakage. Anyhow particle releases can occur near to the connection of the gloves (glove failure) or in case of breach accident. For the particular problem of achieving dynamic confinement at accidental openings, every case has to be examined separately and validated, if

necessary, by an experimental study. The Figure 1 shows a typical glove-box arrangement.

**Figure 1**. Glove-box example

## 3. Experimental benchmark set-up

The experimental test campaign of Whicker and Wasiolek [1] has been used as benchmark. The experimental test room was a modular metal-wall structure with overall dimensions of 4.8 x 6.1 x 2.4(h) m furnished with two mockup glovebox lines and an overhead pass-box (a sealed tunnel used for moving radioactive materials between gloveboxes into the facility). The room supply air was introduced into the room through four 0.2 m diameter inlets located at the ceiling and diffused with 0.3 diameter horizontal deflector (plates) located about 15 cm below each supply inlet. The room air was exhausted through four 0.2 m diameter adjustable flow exhaust register located in the room corners, 0.3 m above the floor. The nominal room air exchange was set to either approximately 6 vol/h (low ventilation LV) and 12 vol/h (high ventilation HV).

Figure 2 shows the aerosol injection and measuring stations (laser particle counter LPC systems) into the experimental room. The particle injection nozzles were adjusted to obtain a low velocity release (approximately 1 cm/s to quickly accommodated the local airflow conditions) of 60 seconds duration ("puff" release). The particle size distribution was approximately log-normal with a count median diameter of 0.52 µm and a geometric standard variation of 2.0. The airflow rate of an LPC was controlled by a critical flow orifice with a sampling rate of about 50 $cm^3/s$.

A commercial sonic anemometer was used to characterized the airflow under the varying conditions. The planes at z=0.6 m, z=1.2 m and z=1,8 m (see the Figure 2 where z=0 represents the floor) were considered to perform the airflow measures. The 19 locations for each of the three planes are described in [1].

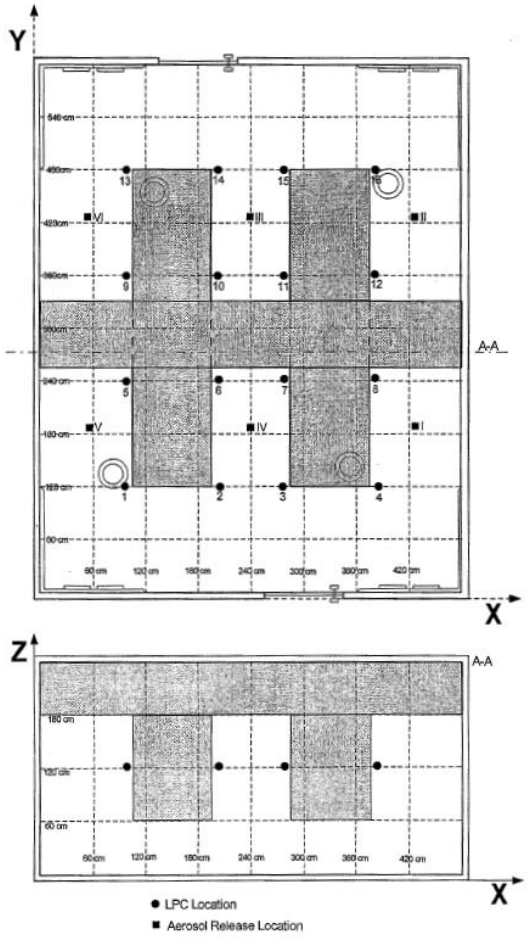


**Figure 2**. Experimental test facility: location of aerosol releases and laser particle counters (LPC)

### 3.1 Metric for particle diffusion

Whicker et al. used lag time and concentration ratio as the metric for comparison particle diffusion between change in release points and the ventilation rates [1]. The lag-time $\boldsymbol{\tau}$ was defined as the time from the start of the release until the time that an aerosol concentration at sample location $\boldsymbol{i}$ exceed three standard deviations above background. The peak concentration was the highest aerosol particle concentration measured during the sampling period. Using these measurements, the concentration ratio for any individual sampling location $\boldsymbol{CR(i)_{20min}}$ was calculated as the ratio of the largest mean peak concentration $\boldsymbol{C_{20min(largest)}}$ measured in the

room divided by each of the mean peak concentrations measured at the other sampling locations $\boldsymbol{C(i)_{peak}}$ during 20 min after the release as shown in the following equation:

$$CR(i)_{20min} = \frac{C_{20\min(largest)}}{C(i)_{20min}} \quad (1)$$

## 4. Numerical model

In this section the governing equations of the numerical model and their boundary conditions are reassumed. The present work makes use the Lagrangian method that can predict the particle distribution in detail but required a considerable computational effort respect to Eulerian approach [6].

### 4.1 Governing equations

The governing equations used during the study are represented by partial differential equations derived by imposing the balance of mass (2), momentum (3) within an infinitesimal element of volume. The last equation (4) represents the Newton's second law applied to each particle. The governing equations, for incompressible and isothermal case are reported in tensor form:

$$\nabla \cdot \boldsymbol{U} = 0 \quad (2)$$

$$\rho \frac{\partial \boldsymbol{U}}{\partial t} + \rho(\boldsymbol{U} \cdot \nabla)\boldsymbol{U} = \nabla \cdot [-p\boldsymbol{I} + \boldsymbol{\tau}] \quad (3)$$

$$\frac{d}{dt}(m_p \boldsymbol{v}) = \left(\frac{1}{\tau_p}\right) m_p(\boldsymbol{u} - \boldsymbol{v}) + m_p \boldsymbol{g} \frac{(\rho_p - \rho)}{\rho_p} + \boldsymbol{F}_{brow} \quad (4)$$

where $\boldsymbol{U}$ is the time average fluid velocity vector (while $\boldsymbol{u}$ is the instantaneous fluid velocity vector), $\boldsymbol{v}$ the particle velocity vector, $\tau_p$ the particle velocity response time (the drag force is modeled using Stokes formulation that takes into account the turbulent dispersion by means of $\boldsymbol{u}'$ which is the turbulent velocity fluctuation), $\boldsymbol{g}$ the gravity vector and $\boldsymbol{F}_{brow}$ is the Brownian force. For the other terms please refer to Comsol Multiphysics Reference Manual.

### 4.2 Boundary conditions

For the first simulation step (fluid flow study), the following boundary conditions has been applied: atmospheric pressure at one of the four ventilation outlet sections (normal flow and no viscous stress option), velocity outlet condition at the other outlet sections, logarithmic wall function on the walls, velocity inlet condition (normal flow velocity) on the entrance of the ventilation ceiling inlets (see Figure 3). From experimental measurements, it has been determined that not all of the four outlets and four inlets exhausted the same amount of air. This finding has been incorporated into the model boundary conditions. The turbulence intensity at the inlets has been assumed equal to 30% even if this experimental value is not available. The volumetric flow aspirated by the LPCs has been neglected in the model.

For the second simulation step (particle tracing study) the particles has been released from the stations I,II and III (see Figure 2 ) at t=0, for 60 seconds, with an initial velocity equal to the experimental case. The outlet sections has been treated by means of freeze condition for the room ventilation grille. Control volumes has been used to count the particles captured by LPCs with particle volume accumulator operator in order to produce an estimate of particle concentration. The other surfaces has been modeled with bounce option [6].

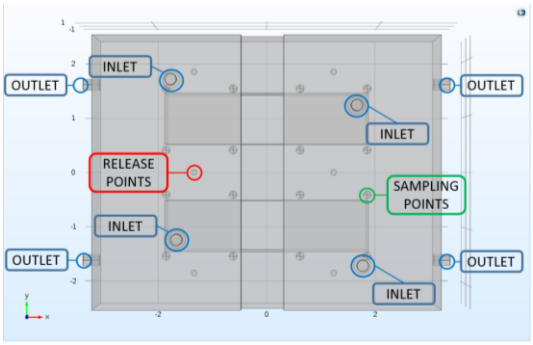


**Figure 3.** Boundary conditions reference scheme

## 5. Use of COMSOL Multiphysics®

With the numerical simulations, they have been firstly evaluated the capabilities of the numerical model to reproduce the available experimental data and secondly they have been defined the optimized positioning of continuous air monitoring to obtain a quickly and good sensitive response.

The 3D simulations have been performed with COMSOL Multiphysics version 5.2, Heat Transfer and Particle Tracing Modules, and they

have been based on the following steps: 1) stationary fluid flow study (single-phase incompressible and isothermal turbulent k- ε closure model); 2) time dependent particle transport study, using the air velocity field obtained in the first study. The particle transport simulation is based on the "sparse flow" approach where the continuous phase affects the motion of particles but not vice versa (one-way coupling). Computations have been carried out for two nominal room air exchange, approximately 6 vol/h (low ventilation LV) and 12 vol/h high ventilation HV) and for three different release locations. The particle aerodynamic equivalent diameter is set to 0.52 µm.

### 5.1 Computational domain and mesh

The geometrical dimensions of the laboratory has been reproduced in 1:1 scale (see Figure 2 and Figure 3). The mesh consists of a tetrahedral network of about 1.940.000 elements with average element quality 0.62 (minimum quality 0.018) for both simulation steps. A finer mesh has been used near the wall in order to guarantee sufficient small values of wall lift-off. The mesh built represents a compromise for obtaining sufficiently accurate results and for a reasonably short simulation time (20 hours for particle study on a workstation Intel Xeon CPU @ 2.40 GHz, 64 GB RAM).

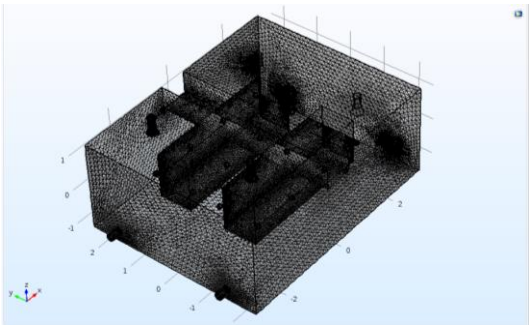

**Figure 4**. Mesh used for both simulation steps

### 5.2 Solver set-up for fluid flow study

The stationary fluid flow study has been used to obtain the velocity field inside the laboratory. The physics selected has been single phase turbulent flow k-ε formulation as closure model (wall function). As described in § 4.1 the flow has been considered incompressible and isothermal. The direct, MUMPS, segregated solver configuration has been used during the simulation. The solution has been considered to be converged when the residual values fell below less than $10^{-6}$ (relative and absolute tolerance).

### 5.3 Solver set-up for particle transport study

Transient calculations of the aerosol dispersion over a twenty minute period have been performed, and aerosol concentration versus time has been recorded at sixteen experimental sampling locations (LPCs). The transient newtonian formulation has been employed with Stokes drag law implementation. As described in § 4.1 the forces considered were the drag, the gravity and Brownian ones. They have been performed six computational studies that represent the combinations of three different release locations and two ventilation configurations (low and high exchange ratio). The transient simulations have been extended for a simulation time of 1200 seconds. The lag time and the concentration ratio have been evaluated statistically by tracking a large number of particles. Based on previous study [8] 60.000 particles were found to be sufficient to give results independent of the number of particles. The direct, MUMPS, fully-coupled solver configuration has been used during the simulation. The solution was considered to be converged when the residual values fell below less than $10^{-3}$ (relative and absolute tolerance).

## 6. Results

The paragraph 6.1 shows the capabilities of the numerical model to reproduce the available experimental data for the ventilation fluid flow whereas in § 6.2 are summarized the performances in terms of particle diffusion.

### 6.1 Fluid flow

Velocity field in vertical slices, obtained from the steady-state CFD solution, are shown in Figure 5 for the case of 6 vol/h. High velocities are noticed at the inlets, at the outlets and along the ceiling and room walls. The flow in the room is undesirable from the standpoint of worker safety due to the presence of inlet plate deflectors that impose a tangential recirculation instead of a downward flux (most protective airflows pattern would sweep aerosol downward and away from the breathing zone). Velocities as high as 1.6 m/s at the inlets are recorded, but in general the velocities are in the 0.05 m/s range (for the case of 6 vol/h). The comparison between the computer simulations and the available

experimental results are shown in Figure 6. The histogram graph that represents the average magnitude velocities calculated at planes z=0,6, z=1,2 and z=1,8 m shows good agreement with experimental dates. The differences could be explained considering that the numerical averages are computed on surface (plane) whereas the experimental values on the 19 sampling stations.

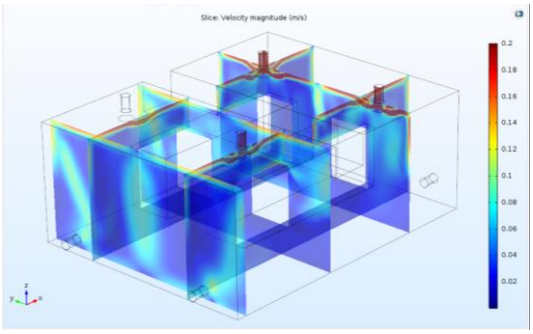


**Figure 5**. Slices of velocity magnitude for 6 vol/h

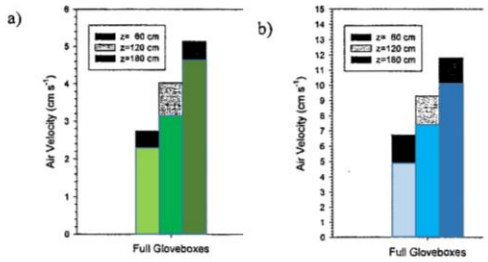


**Figure 6**. Comparison of experimental and numerical results: average magnitude velocities for 6 vol/h, case a), on the left and for 12 vol/h, case b), on the right

Whicker's test campaign measures confirm that the turbulence was approximately isotropic for each ventilation condition and that the mean values of the turbulence intensities are near to 30% regardless of ventilation conditions [4]. Figure 7 and Figure 8 display the turbulence intensity isosurfaces for 6 vol/h and 12 vol/h room air exchange respectively. The mean value of turbulence indicated by Whicker seems to be a little bit excessive, in particular for 6 vol/h condition, even if the turbulence intensity at the inlets, during numerical simulations, has been forced to 30%. With numerical simulations a laminarization process seems to occur for 6 vol/h and only in few points the turbulence intensity is above to 2%. For 12 vol/h exchange ratio at some points, mainly around the edges, the turbulence intensity reaches 20%. The turbulence intensity plays an important role on the particle diffusion and this aspect has to be considered analyzing the results of the second simulation step.

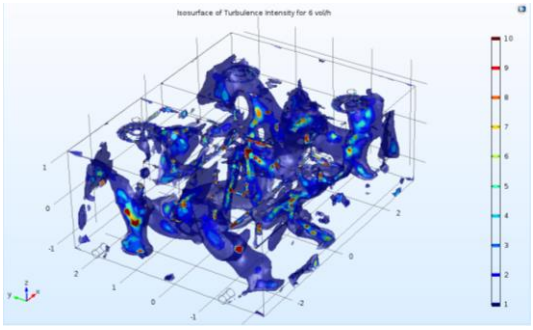


**Figure 7**. Turbulence intensity isosurface for 6 vol/h

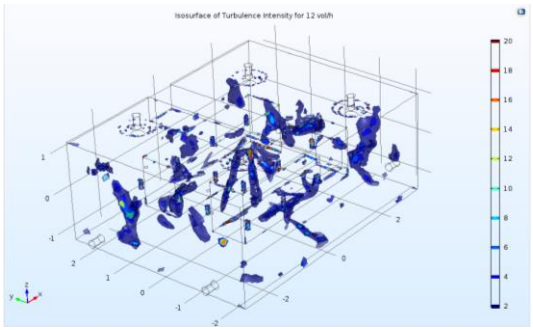


**Figure 8**. Turbulence intensity isosurface for 12 vol/h

### 6.2 Particle diffusion

The steady-state CFD solution has been used as input in solving dispersion patterns for the aerosol releases. The figure 9 shows the particle trajectories for the release from the station I, for the low exchange ratio value.

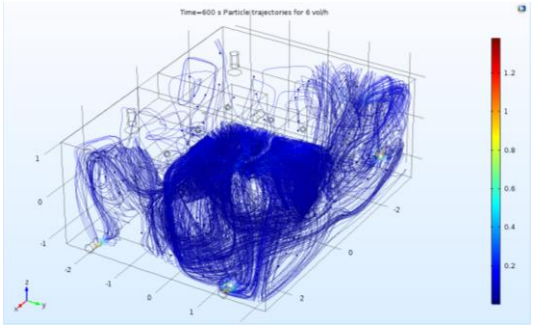


**Figure 9**. Particle trajectories for the release from station I and 6 vol/h

Transient calculations of the aerosol dispersion by advection, turbulent diffusion, and molecular diffusion over a twenty-minute period

have been performed, and aerosol concentration (number of particles into the control volumes) versus time has been recorded at sixteen sampling locations. An example of this kind of graph is shown in Figure 10, where is indicated the concentration time history at LPC station n. 8 due to the aerosol release from station I. In the Figure are highlighted the metric used for the particle transport study: the lag-time and the peak concentration, expressed by the total number of particles inside the control volume (sphere) useful to calculate the concentration ratio.

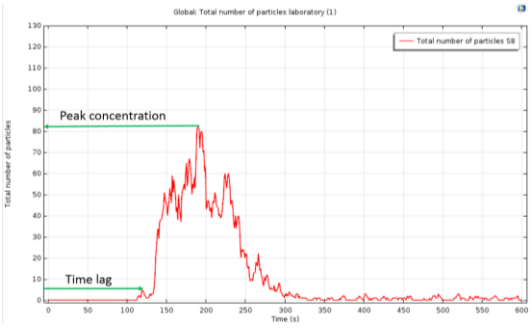


**Figure 10.**Concentration time history for LPC station 8, release station I and 6 vol/h exchange

The Figure 11 reassumes the comparison between the experimental and the numerical results in terms of lag time and concentration ratio.

FB-LV

| Release location | Lag time mean (s) ± SEM | | Mean $CR_{20\text{-}min}$ ± SEM | | Mean $CR_{peak}$ ± SEM |
|---|---|---|---|---|---|
| I | 223 ± 24 | 215 | 27 ± 8 | 23 | 69 ± 21 |
| II | 135 ± 20 | 195 | 13 ± 4 | 10 | 14 ± 4 |
| III | 159 ± 24 | 218 | 26 ± 9 | 26 | 66 ± 26 |
| IV | 83 ± 10 | | 4 ± 1 | | 20 ± 5 |
| V | 123 ± 20 | | 11 ± 3 | | 42 ± 13 |
| VI | 187 ± 28 | | 33 ± 10 | | 85 ± 26 |
| Avg: | 152 | | 19 | | 49 |
| SD | 49 | | 11 | | 29 |

FB-HV

| Release location | Lag time mean (s) ± SEM | | Mean $CR_{20\text{-}min}$ ± SEM | | Mean $CR_{peak}$ ± SEM |
|---|---|---|---|---|---|
| I | 71 ± 10 | 105 | 6 ± 1 | 4.5 | 18 ± 5 |
| II | 63 ± 8 | 80 | 3 ± 0.4 | 3.5 | 10 ± 2 |
| III | 71 ± 9 | 100 | 4 ± 1 | 6 | 16 ± 4 |
| IV | 88 ± 11 | | 9 ± 2 | | 52 ± 15 |
| V | 79 ± 10 | | 8 ± 2 | | 22 ± 7 |
| VI | 78 ± 10 | | 9 ± 2 | | 22 ± 6 |
| Avg: | 75 | | 7 | | 23 |
| SD | 9 | | 3 | | 15 |

**Figure 11.**Comparison of experimental and numerical results for particle tracing study. The upper table refers to low ventilation scenario, the lower to the high ventilation.

Except for the release stations II and III in low ventilation condition the lag-time are well reproduced. Fewer difficulties can be observed for the concentration ratios in particular for low ventilation case. The introduction into the model of the mass flow handled by the LPC could reproduce the transport of particles with even more reliability.

### 6.3 CAM placement strategy

The numerical aerosol tracer release study can provide the lag time and the concentration ratio parameters for each combination of release and sampling locations investigated. A possible strategy to define the optimized sampling locations starts with the building of the matrix $M(i,j)$ of equation (5):

$$M(i,j) = \frac{CR(i,j)_{peak}}{\tau(i,j)} \qquad (5)$$

where i is the sampling location and j is the release location studied. The second step is to put the rows in decreasing order based on the sum of their elements obtaining the optimized matrix $OM(i,j)$. The best one sampling location is represented by the positioning expressed by the first row, the best two sampling locations by the positioning of the first and the second rows and so on.

## 7. Conclusions

Computed and measured ventilation fluidynamical characteristics and aerosol concentration time history data are compared and shows general agreement.

The study also confirms that laboratory with higher ventilation rates provide more mixing of release aerosol trough the space.

A CAM placement strategy is defined in order to select the best locations that are generally "downwind" of the release points.

The introduction into the model of the mass flow handled by the LPC could reproduce the transport of particles with even more reliability.

Evaluation of aerodynamic diameter effects on particle diffusion is an important area for further investigations.

## 8. References

1. J. Whicker, P. Wasiolek, "Influence of room geometry and ventilation rate on airflow and aerosol dispersion: implication for worker protection", *Health Physics* **82(1)**:52-63 (2002)

2. J. Whicker, J. Rodgers, “A quantitative method for optimized placement of continuous air monitors”, *Health Physics* **85(5)**:599-609 (2003)
3. J. Whicker, J. Rodgers, “Evaluation of continuous air monitor placement in a plutonium facility”, *Health Physics* **72(5)**:734-743 (1997)
4. J. Whicker, “Implications of Room Ventilation and Containment Design for Minimization of Worker Exposure to Plutonium Aerosols”, *Los Alamos National Laboratory Annual Report*, 1999
5. S. Konecni, J. Whicker, “Computational modeling and experimental characterization of indoor aerosol transport”, *Proceedings of ASME FEDSM 2002*
6. Z. Zhang, Q. Chen, “Experimental Measurements and Numerical Simulations of Particle Transport and Distribution in Ventilated Rooms”, *Atmospheric Environment*, **40(18)**, 3396-3408
7. S. Konecni, J. Whicker, “Monitoring Dispersion Of Aerosols In Work Rooms Using Computational Fluid Dynamics”, *Proceedings of ASME FEDSM00***,** 2000
8. Z. Zhang, Q. Chen, “Comparison of the Eulerian and Lagrangian methods for predicting particle transport in enclosed spaces”, *Atmospheric Environment*, 2006
9. Z. Chen, S. Konecni, “Computational Modeling and analysis of airflow in a tritium storage room”, *Los Alamos National Laboratory*, Proceedings of FEDSM’03, 2003